EUROfusion

WPHCD-CPR(17) 17479

R Ragona et al.

Study of a distributed ICRF antenna system for DEMO

Preprint of Paper to be submitted for publication in Proceeding of 22nd Radiofrequency Power in Plasmas Topical Conference (RFPPC 2017)

This work has been carried out within the framework of the EUROfusion Consortium and has received funding from the Euratom research and training programme 2014-2018 under grant agreement No 633053. The views and opinions expressed herein do not necessarily reflect those of the European Commission.

Study of a distributed ICRF antenna system in DEMO

Riccardo Ragona[1,2,*] and *Andre* Messiaen[1]

[1]Laboratory for Plasma Physics, Royal Military Academy, (LPP-ERM/KMS), BE-1000, Brussels, Belgium
[2]Ghent University, Department of Applied Physics, 9000 Ghent, Belgium

Abstract. An ICRF distributed antenna integrated in the blanket of the DEMO reactor is presently considered as a candidate IC system to heat the central plasma core without density cut-off. Lower power density is envisaged for not exceeding the voltage standoff due to the large coupling evanescent length. Different options for the antenna array(s) and for the feeding schemes are compared, based on detailed circuital modelling. Voltages and currents (amplitude and phase) are computed for each element of the array and the power delivered by each feeding scheme is evaluated allowing to study the different characteristics of each system. The results can be scaled to an arbitrary large number of straps and feeding connections.

1 Introduction

Three different feeding cases are analysed: (i) an array with resonant ring recirculation feeding system [1], (ii) an array with periodic conventional feeding [2] and (iii) an array with all elements fed [3]. We first analyse the last case, that is the one with the best possible performances [4] although with the drawback of requiring a large number of mutually coupled feeding lines. In the second case the dependency of the response of the structure with different relative phasing of the generators is analysed and the power capabilities are studied. In the end an array fed with one resonant ring is compared to the traveling wave array (TWA) of [1] and a general case of two consecutive resonant rings is studied. Conclusions are then presented.

2 Analysis

2.1 Simulation parameters

All the three cases analysed are based on an array of 28 elements, N_{str}=28. In Fig. 1 the array is presented in one of the feeding configuration analysed (case (ii)). This system can be described by a predominantely diagonal matrix with some elements at the upper right and lower left corners due to the symmetry of the system. Here only the mutual coupling with the first two neighbours are considered. Exploiting the symmetry of the system means that all values of the self-inductance L_i=L and mutual couplings M_{i+1}=M_1, M_{i+2}=M_2 are respectively the same, for i=1,..,N_{str}, and all other elements of the strap impedance matrix $\mathbf{Z}_s$ are equal to zero. At a frequency f_0=50MHz, being ω_0=2πf_0 the angular frequency, $\omega_0 L$=56Ω, $\omega_0 M_1$=17.3Ω and $\omega_0 M_2$=7.25Ω. A resistance R_i=R=2.5Ω is added in series to each strap to account, in an appropriate way, for the coupling of power to the plasma. This arbitrary value is choosen as reference to compare the different cases and it is not consistently derived from a coupling code (e.g. ANTITER [5]). The array is configured as combline with a tuning reactance on each strap and can be described by an array impedance matrix $\mathbf{Z}_a$ such that $1/\mathbf{Z}_a = 1/\mathbf{Z}_s+1/\mathbf{Z}_c$ where $1/\mathbf{Z}_c$ is the admittance matrix of the tuning capacitors. The details of the modelling procedure are explained in [4]. It is worth to remind that, in its passband, the combline acts as transmission line with characteristic impedance Z_0=Z_{it} [1] where Z_{it} is the iterative impedance of the structure [6].

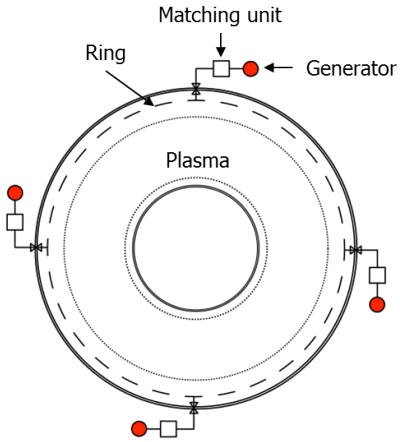

Fig. 1. Sketch of the array fed as described in section 2.3.

2.2 360° array – all straps fed

A continuous array distributed 360° all around the machine is fed at each element by an independent generator connected through its own matching-decoupling network [3]. The generators are feedback controlled to provide the same strap current amplitude $|I_s|$=178A with a phase difference Δϕ between elements such that the peak of the spectrum is centered on $k_{z,M} = p$

* Corresponding author: riccardo.ragona@rma.ac.be

$k_{z,M0}$. The index p represents the harmonic number of $k_{z,M0} = 2\pi/(N_{str}S_z)$ where the denominator is the perimeter of the array being S_z the inter-strap distance, i.e. the distance between the centre of two consecutive elements. For S_z=0.3m, $k_{z,M0}$ =0.748m^{-1} and for the harmonic p=5 we get $k_{z,M}$ = 3.74m^{-1} with for each strap the following values of maximum voltage $|V_{str}|$ = 11.09kV, of input impedance and input current respectively Z_{in} = (187+i503)Ω and $|I_{in}|$ = 20.67A seen and provided by the generators. The input current is given by the sum of the current on the strap and the one in the tuning capacitor: $I_{in} = I_s + I_c$.

In Fig. 2, the value of the input impedance of the array is computed for the discrete set of $k_{z,M}$, each of those choosen by a different Δϕ (represented by the dots). The computation for a continuous spectrum of $k_{z,M}$ (lines) reveals a resonance in the input impedance when $k_{z,M}$ is equal to the one obtained by the dispersion relation of the traveling wave structure at the tuned frequency f_0. For this value we have a minimum amplitude of the input current required to obtain the requested strap current.

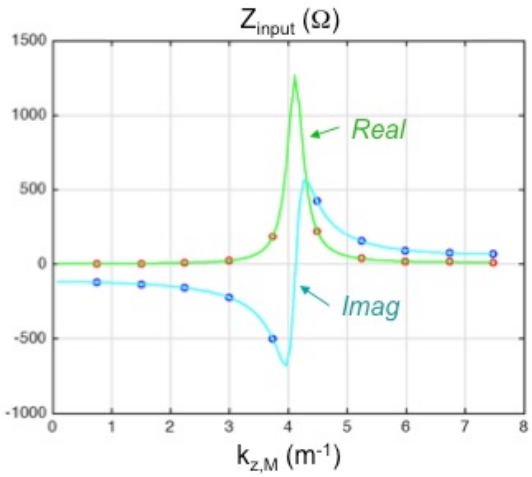

Fig. 2. Input impedance for different spectra peak positions.

Unfortunately the system is not load resilient. A variation of the plasma loading on the antenna, or a failure of one generator, will lead to a change in the input impedance of the neighbouring generators causing an important power imbalance. The result is that one or both neighbours will be mismatched and receive a large amount of reflected power that will activate the safety protection chain tripping the power source.

2.3 360° array – periodic feeding

A possible way to reduce the number of feeding lines is to provide periodic feeding to the 360° array. Here we analyse a case where the array is fed with 4 independent generators evenly distributed (depicted in Fig. 1) and connected to the elements 1, 8, 15 and 22. Two different phasing cases for the generators are studied: (A) $\Delta\theta = \pi$ and (B) $\Delta\theta = \pi/2$. The resulting excitation spectra are shown in Fig. 3 where the reader will recognised the shape with two main peaks typical of case (A). From the point of view of traveling waves, (A) corresponds to the case in which two opposite directed traveling waves interfere leading to a standing wave pattern. To be noted the absence of coaxial modes (k_z<k_0) excitation. The voltage amplitude distribution on each strap appears to vary considerably and it is shown in Fig. 4 for an applied forward voltage of V_+ = 10kV. A nice symmetric behaviour emerges from the graph for both cases.

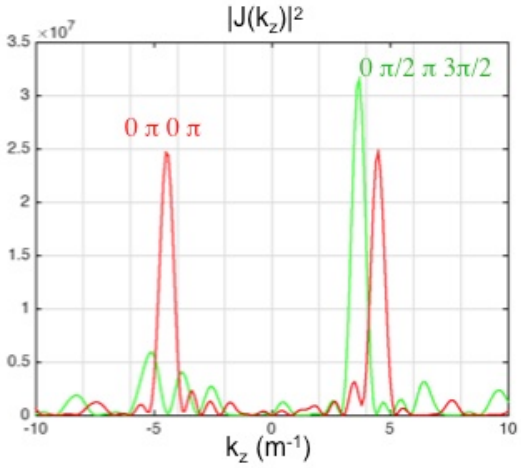

Fig. 3. Spectrum of the two cases for the array periodically fed in the conventional way with self-tuned elements.

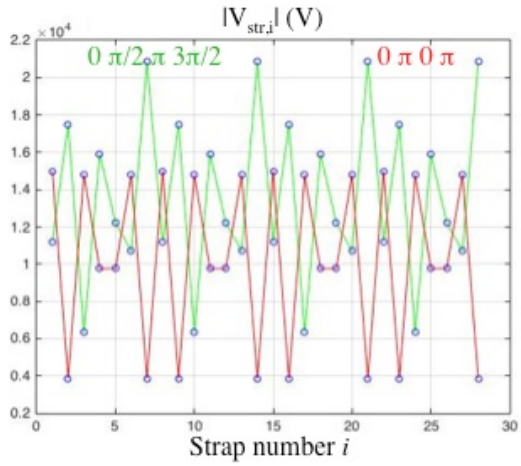

Fig. 4. Voltage amplitude along the array for the two cases considered.

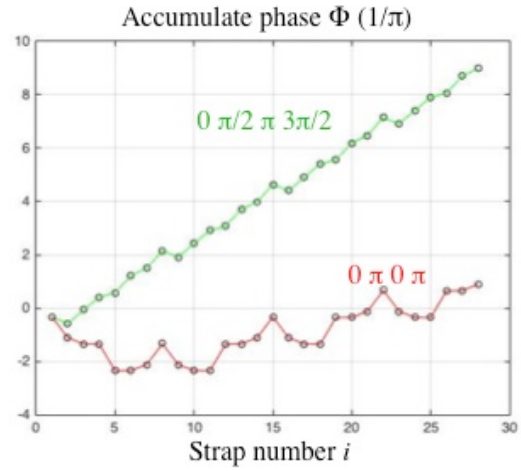

Fig. 5. Phase along the array for the two cases considered.

The current amplitude distribution presents the same characteristics of the voltage one. The value of the phase at each strap is shown in Fig. 5.

The array impedance matrix $\mathbf{Z}_a$ reveals the strong coupling between the fed elements (i.e. #1, #8, #15 and #22) connected to the 4 generators. The characteristic impedance of the ring is $Z_{0,a} = 69\Omega$. The contribution of each generator to the active power provided by the 4 fed elements is given by the power matrix $\mathbf{P}_A$ and $\mathbf{P}_B$ for the two different cases analysed.

$$\mathbf{Z}_a = \begin{vmatrix} 42.11 - i6.29 & -13.76 - i36.81 & 2.04 + i49.39 & -13.76 - i36.82 \\ -13.76 - i36.81 & 42.11 - i6.29 & -13.76 - i36.81 & 2.04 + i49.39 \\ 2.04 + i49.39 & -13.76 - i36.81 & 42.11 - i6.29 & -13.76- i36.81 \\ -13.76 - i36.81 & 2.04 + i49.39 & -13.76 - i36.81 & 42.11 - i6.29 \end{vmatrix}$$

The real part of the two power matrices is:

$$\mathrm{Re}(\mathbf{P}_A) = \begin{vmatrix} 2.521 & 0.824 & 0.122 & 0.824 \\ 0.824 & 2.521 & 0.824 & 0.122 \\ 0.122 & 0.824 & 2.521 & 0.824 \\ 0.824 & 0.122 & 0.824 & 2.521 \end{vmatrix} 100\mathrm{kW}$$

$$\mathrm{Re}(\mathbf{P}_B) = \begin{vmatrix} 5.616 & 4.911 & -0.271 & -4.911 \\ -4.911 & 5.616 & 4.911 & -0.271 \\ -0.271 & -4.911 & 5.616 & 4.911 \\ 4.911 & -0.271 & -4.911 & 5.616 \end{vmatrix} 100\mathrm{kW}$$

where each generator is delivering respectively $P_{G,A}$ = 429kW or $P_{G,B}$ = 534kW giving rise to total power levels of $P_{tot,A}$ = 1.72MW for case (A) and $P_{tot,B}$ = 2.14MW for case (B).

2.4 360° array – consecutive resonant rings

The same circular array of the previous examples is fed firstly by only one resonant ring circuit and then by two consecutive ones (Fig. 9). A TWA fed by a resonant ring system was analysed in [1] and will be compared with the first case where the resonant ring is connected to two arbitrary but consecutive elements i and i+1, e.g. #28 and #1. The main difference with a normal TWA section is the mutual coupling between the inputs of the circuit due to the circular symmetry of the ring. This leads to a substantial differences in the array behaviour: (i) a different characteristic impedence of the array $Z_0 = Z_{it}$ and (ii) a much larger voltage and current amplitudes variation compared to the exponential decay of the single section. An example of the amplitude of the voltage is shown in Fig. 6. The parameters are: $Z_{0,r} = 85\Omega$ for the ring, $Z_{0,s} = 148\Omega$ for the section and $V_{G+} = 10$kV. The forward power is then computed by $P_+ = 0.5|V_{G+}|^2/Z_0$, i.e. $P_{+r} = 588$kW and $P_{+s} = 338$kW. The linear phase variation along the array is however preserved (see Fig. 7). As a consequence the spectra for the cases assumes the shape shown in Fig. 8 where in the case of the ring a backward component appears sign of a wave traveling in the opposite direction, injected in the line due to the mutual coupling between the inputs.Both the section and the ring maintain the capability of controlling the position of the peak varying the frequency.

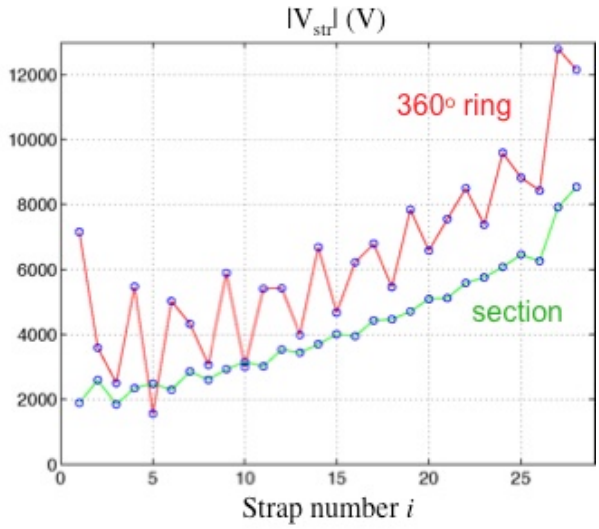

Fig. 6. Voltage amplitude along the array for the two cases considered and for a generator forward voltage V_{G+}=10kV.

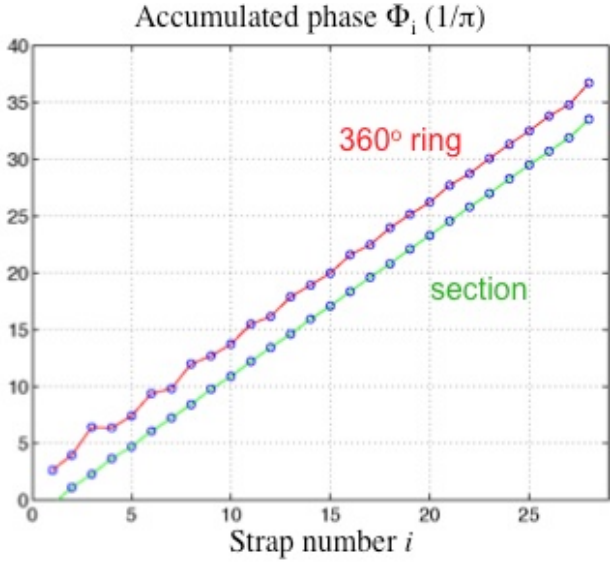

Fig. 7. Phase along the array for the ring and for the section.

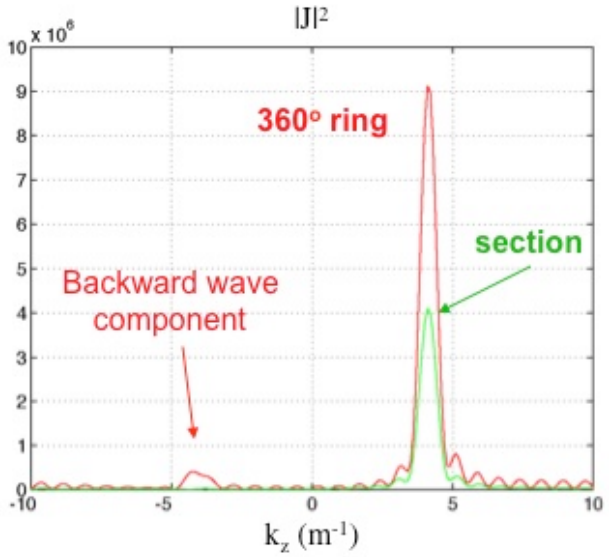

Fig. 8. Spectra for the ring and for the section.

The second case consists of the same ring fed by two consecutive resonant ring (see Fig. 9), connected symmetrically at the elements 1, t, u and v. As seen above, there is mutual coupling between the output (e.g. 1, u) and the input (e.g. t, v) of the two resonant ring feeding systems due to the terms $\mathbf{Z}(1,v)$, $\mathbf{Z}(v,1)$, $\mathbf{Z}(t,u)$ and $\mathbf{Z}(u,t)$ of the array impedance matrix $\mathbf{Z}_a$. For our particular case: $v = 28$, $u = 15$ and $t = 14$.

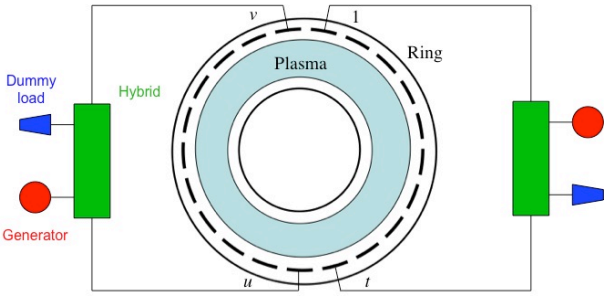

Fig. 9. Ring array fed by to consecutive resonant ring.

Also in this case the voltage amplitude presents large fluctuations, shown in Fig. 10, due to the interference of opposite directed traveling waves that manifests itself again in the spectrum, like for the case in Fig. 8. But here, due to the strong modulation of the current on the straps, side peaks appear in the spectrum as shown in Fig. 11.

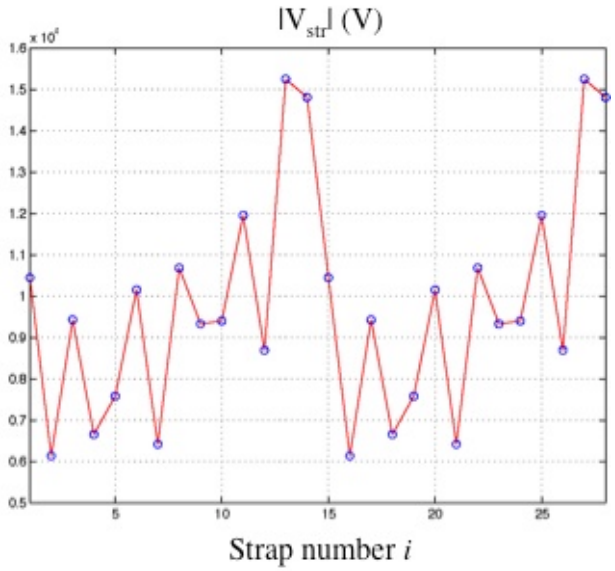

Fig. 10. Voltage amplitude along the array for the two cases considered and for a generator forward voltage V_{G+}=10kV.

The real part of the power matrix for this case is:

$$\mathrm{Re}(\mathbf{P}_A)= \begin{vmatrix} 1.615 & -1.046 & -0.078 & -4.807 \\ 1.006 & 4.474 & 4.646 & -0.217 \\ -0.078 & -4.807 & 1.615 & -1.046 \\ 4.646 & -0.217 & 1.006 & 4.474 \end{vmatrix} \text{100kW}$$

that gives $P_1 = P_{15} = -432$kW, $P_{14} = P_{28} = 991$kW. The first two values indicates that the power is extracted from the structure and recirculated in each resonant ring. The total power delivered by the array is $P_{tot} = 1.18$MW.

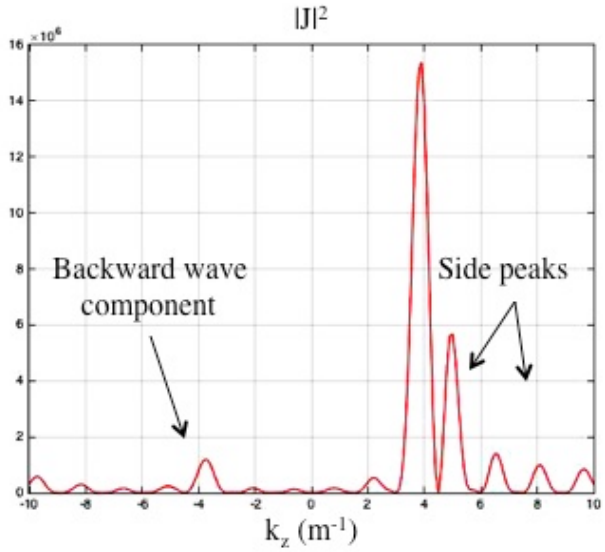

Fig. 11. Spectrum for the ring fed by two consecutive resonant ring systems.

3 Conclusions

The analysis presented shows that the preferred system for DEMO is the self-tuned strap array sections fed in resonant ring configuration (Fig. 9). It has the advanges of: (i) best selective excitation spectrum, (ii) load resilience, (iii) simplicity of its adjustement and (iv) no expected mutual coupling between adjacent sections. Moreover, a configuration with separate sections, ideally one per each sector of the machine, provides better reliability than all other solution: if one element (or one generator) of one section fails, the other ones will not be significantly affected. The second layout that provides excellent rf performances is the 360° ring array with each strap fed independently. For this system, the problems of load resilience and mutual coupling between feeding networks are not yet solved and all solutions based on a complete 360° strap ring suffer from mutual coupling between the feeding networks and from standing waves along the TWA structure.

This work has been carried out within the framework of the EUROfusion Consortium and has received funding from the Euratom research and training programme 2014-2018 under grant agreement No 633053. The views and opinions expressed herein do not necessarily reflect those of the European Commission.

References

1. R. Ragona and A. Messiaen, Nucl. Fusion **56** (2016) 076009.
2. G. Bosia, Fus. Eng. and Design **92** (2015) 8-15.
3. G. Bosia and R. Ragona, this conference.
4. A. Messiaen and R. Ragona, this conference.
5. A. Messiaen et al, Nucl. Fusion **50** (2010) 025026.
6. C. G. Montgomery, R. H. Dicke, and E. M. Purcell. *Principles of Microwave Circuits*, volume 8 of *MIT Radiation Laboratory Series*. McGraw-Hill, New York, 1948